Thermal analysis of intense femtosecond laser ablation of aluminum*

Hu Hao-Feng(胡浩丰)[a)], Ji Yang(吉 扬)[b)], Hu Yang(胡 阳)[b)],
Ding Xiao-Yan(丁晓雁)[b)], Liu Xian-Wen(刘贤文)[b)], Guo Jing-Hui(郭静慧)[c)],
Wang Xiao-Lei(王晓雷)[a)†], and Zhai Hong-Chen(翟宏琛)[a)‡]

[a)] *Institute of Modern Optics, Key Laboratory of Optoelectronic Information Science & Technology, Ministry of Education, Nankai University, Tianjin* 300071, *China*

[b)] *College of Precision Instruments and Optoelectronics Engineering, Tianjin University, Tianjin* 300072, *China*

[c)] *College of Information Technical Science, Nankai University, Tianjin* 300071, *China*

(Received 28 May 2010; revised manuscript received 15 July 2010)

This paper numerically simulates the process of ablation of an aluminum target by an intense femtosecond laser with a fluence of 40 J/cm^2 based on the two-temperature equation, and obtains the evolution of the free electron temperature and lattice temperature over a large temporal and depth range, for the first time. By investigating the temporal evolution curves of the free electron temperature and lattice temperature at three representative depths of 0, 100 nm and 500 nm, it reveals different characteristics and mechanisms of the free electron temperature evolution at different depths. The results show that, in the intense femtosecond laser ablation of aluminum, the material ablation is mainly induced by the thermal conduction of free electrons, instead of the direct absorption of the laser energy; in addition, the thermal conduction of free electrons and the coupling effect between electrons and lattice will induce the temperature of free electrons deep inside the target to experience a process from increase to decrease and finally to increase again.

Keywords: femtosecond laser ablation, two-temperature equation, finite difference method, thermal conduction of free electrons

PACS: 42.62.–b, 66.10.C–, 63.20.kd **DOI:** 10.1088/1674-1056/20/4/044204

1. Introduction

Laser ablation is a complicated process that involves various physical mechanisms depending on both laser parameters and target properties, of which the temperature is an important physical parameter in the ablation process and will affect the physical mechanisms and the morphologies of microstructures induced by the laser ablation. Up to now, researchers in related fields have made some numerical calculations of the temperature characteristic during the ablation process,[1−4] and based on those calculations, the ablation rate, electron diffusion kinetics, electron–phonon coupling time, and thermal incubation effect closely related to the ablation process have been investigated, which, however, are mainly focused on the temperature of the material on the target surface within a short time duration. While for the intense femtosecond laser ablation with high fluences, the ablation depth can reach a scale of micrometer,[5,6] and thus the thermal effect beneath the surface will be of great interest to be investigated. On the other hand, due to the ultrashort pulse duration and the ultrahigh peak power of the intense femtosecond laser, the electron–phonon coupling time will be much longer than the pulse duration.[3] Further studies, therefore, are needed to identify the thermal process over a large temporal range.

In this paper, the process of intense femtosecond laser ablation of an aluminum target at a fluence of 40 J/cm^2 is numerically simulated based on the two-temperature equation. The calculation results show that the characteristics and physical mechanisms of electron temperature evolution at different depths are different, which is supported by the calculation results obtained at depths of 0, 100 nm and 500 nm, respec-

*Project supported by the National Natural Science Foundation of China (Grant Nos. 10904079 and 60838001), the Specialized Research Fund for the Doctoral Program of Higher Education of China (Grant No. 20090031120041), and the Natural Science Foundation of Tianjin (Grant No. 10JCYBJC01300).

†Corresponding author. E-mail: wangxiaolei@nankai.edu.cn

‡E-mail: zhai@nankai.edu.cn

© 2011 Chinese Physical Society and IOP Publishing Ltd

tively.

2. Simulation model

Two-temperature model[7] were first pointed out by Anisimov, which describes the mechanism of the ultrashort laser pulse interaction with metals. The ablation process can be divided into two stages: at the first stage, the laser energy is absorbed by free electrons; at the second stage, the free electrons transfer the energy to the lattice. Since heat diffuses much faster through the electron subsystem, the lattice thermal conductivity can be neglected.[1] Therefore, the expression of the two-temperature equation in this paper is as follows,

$$C_{\mathrm{e}}\frac{\partial}{\partial t}T_{\mathrm{e}} = \frac{\partial}{\partial z}k_{\mathrm{e}}\frac{\partial}{\partial z}T_{\mathrm{e}} - G(T_{\mathrm{e}} - T_{\mathrm{l}}) + Q(z,t), \quad (1)$$

$$C_{\mathrm{l}}\frac{\partial}{\partial t}T_{\mathrm{l}} = G(T_{\mathrm{e}} - T_{\mathrm{l}}), \quad (2)$$

where t is the time, z is the depth, T_{e}, T_{l}, C_{e} and C_{l} are the temperatures and the volumetric heat capacities of electrons and lattice, respectively, k_{e} is the electron thermal conductivity, and G is a parameter characterizing the electron–lattice coupling. The laser energy source term $Q(z, t)$ is given by

$$Q(z,t) = \sqrt{\frac{\beta}{\pi}}\frac{(1-R)\,J_0}{t_{\mathrm{p}}z_{\mathrm{s}}}\exp\left[-\frac{z}{z_{\mathrm{s}}} - \beta\left(\frac{t-2t_{\mathrm{p}}}{t_{\mathrm{p}}}\right)^2\right], \quad (3)$$

where R is the surface reflectivity, J_0 is the fluence of the laser, z_{s} is the absorption depth, and β is a constant of 4ln2. The initial condition is $T_{\mathrm{e}}(z,0) = T_{\mathrm{l}}(z,0) = T_0$, and the boundary condition is $q_{\mathrm{e}}(0,t) = q_{\mathrm{e}}(L,t) = 0$, where the heat flow of free electron is given by

$$q_{\mathrm{e}} = -k_{\mathrm{e}}\frac{\partial}{\partial z}T_{\mathrm{e}}.$$

The expression of the implicit difference scheme of the two-temperature equation is

$$\begin{aligned} C_{\mathrm{e}j}&\frac{T_{\mathrm{e}j}^{n+1} - T_{\mathrm{e}j}^{n}}{t_0} \\ &= \frac{1}{z_0}\left(k_{\mathrm{e}_{j+\frac{1}{2}}} \times \frac{1}{2}\left(\frac{T_{\mathrm{e}j+1}^{n+1} - T_{\mathrm{e}j}^{n+1}}{z_0} + \frac{T_{\mathrm{e}j+1}^{n} - T_{\mathrm{e}j}^{n}}{z_0}\right)\right. \\ &\quad \left. - k_{\mathrm{e}_{j-\frac{1}{2}}} \times \frac{1}{2}\left(\frac{T_{\mathrm{e}j}^{n+1} - T_{\mathrm{e}j-1}^{n+1}}{z_0} + \frac{T_{\mathrm{e}j}^{n} - T_{\mathrm{e}j-1}^{n}}{z_0}\right)\right) \\ &\quad - G\left(T_{\mathrm{e}j}^{n} - T_{\mathrm{l}j}^{n}\right) + Q, \end{aligned} \quad (4)$$

$$C_{\mathrm{l}}\frac{T_{\mathrm{l}j}^{n+1} - T_{\mathrm{l}j}^{n}}{t_0} = G(T_{\mathrm{e}j}^{n} - T_{\mathrm{l}j}^{n}), \quad (5)$$

where

$$k_{\mathrm{e}_{j+\frac{1}{2}}} = k_0\frac{T_{\mathrm{e}j+1}^{n} + T_{\mathrm{e}j}^{n}}{T_{\mathrm{l}j+1}^{n} + T_{\mathrm{l}j}^{n}}$$

and

$$k_{\mathrm{e}_{j-\frac{1}{2}}} = k_0\frac{T_{\mathrm{e}j-1}^{n} + T_{\mathrm{e}j}^{n}}{T_{\mathrm{l}j-1}^{n} + T_{\mathrm{l}j}^{n}}.$$

3. Results and discussion

The aluminum is chosen to be the ablation target, and its parameters are given as follows: the thermal conductivity $k_0 = 2.36$ W/m^3·K; $G = 7.05 \times 10^{16}$ W/m^3·K; the volumetric heat capacities of electrons is given by $C_{\mathrm{e}} = C_{\mathrm{e}0}T_{\mathrm{e}}$, where $C_{\mathrm{e}0} = 91$ J/cm^3·K^2; $C_{\mathrm{l}} = 2.41$ J/m^3·K; the surface reflectivity R is chosen to be 0.1; the fluence J_0 is chosen to be 40 J/cm^2; the pulse width $t_{\mathrm{p}} = 50$ fs; the absorption depth $z_{\mathrm{s}} = 1/\alpha$, where the absorption coefficient $\alpha = 1.3 \times 10^8$ m^{-1}.

Based on the simulation results, we find that the evolutions of the electron temperature in three depth regions are different, and the result at depths of 0, 100 nm and 500 nm is chosen to illustrate the thermal process in the corresponding depth region, respectively.

3.1. Investigation of the aluminum target surface

The surface electron temperature and lattice temperature versus time are investigated first of all, as shown in Fig. 1. During the pulse duration, surface electrons directly absorb the laser energy and are rapidly heated up to 4.8×10^5 K. After the laser pulse, on the one hand, the free electrons transfer the energy to lattice owing to the electron–phonon coupling; and on the other hand, the heat flow of the surface electrons directs to the inner part of the target. The former leads to an increase in the lattice temperature and both the free electrons and surface electrons lead to a decrease in the electron temperature. Therefore, the electron temperature and lattice temperature tend to be uniform gradually and become the same value at 100 ps, as shown in Fig. 1. The electron–phonon coupling terminates at this time, which is considered to be the electron–phonon relaxation time, which is much longer than the pulse duration in our case. Therefore, this ablation process is nonequilibrium,[8] which is different from the ablation by the laser with a long pulse duration. After the process of electron–phonon coupling, the material on the target surface will transfer the heat to the inner part of the target continuously,

resulting in a decrease in the electron temperature and lattice temperature at the surface, as shown in Fig. 1.

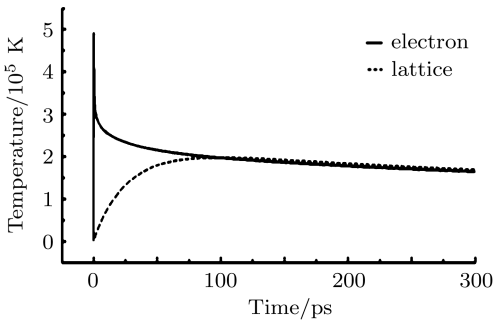


Fig. 1. Surface electron and surface lattice temperature as a function of time heated by a laser pulse with $t_{\rm p}$ of 50 fs and J_0 of 40 J/cm^2.

3.2. Investigation at different depths inside the target

The energy transfer inside the target during the ablation process is more complicated in comparison with that at the target surface. In particular, in addition to the absorption of the laser energy and the electron–phonon coupling, the energy transfer between the electrons at different depths also needs to be taken into account. Since the thermal process is irrelevant to the energy source after the laser pulse, isolating the effect of the laser pulse enables us to quantitatively analyse the thermal effect induced by the energy source and subsequently induced by the thermal conduction and electron–phonon coupling, respectively. Therefore, it is helpful for us to further understand the evolution of the material temperature.

The inset of Fig. 2 shows the energy source term Q at the target surface as a function of time. It is noticed that the energy source term is nearly 0 at 200 fs, and therefore the irradiation time of the laser pulse can be considered to be 200 fs. Figure 2 shows the electron temperature and lattice temperature as a function of depth at the end of the pulse (at 200 fs). It can be seen from Fig. 2 that the electron temperature decreases sharply with the increase in the depth, and it reaches 300 K at a depth of 210 nm. During the irradiation time of the laser pulse, the thermal conduction of the electrons is minor in comparison with the direct absorption of the laser energy by the laser pulse, and thus it can be neglected within the pulse duration.[9] Therefore, the result in Fig. 2 approximately represents the temperature increase induced by the absorption of the laser energy.

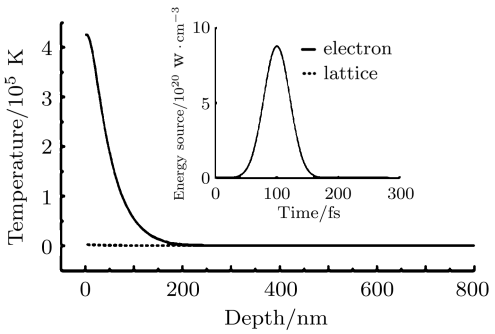


Fig. 2. Electron temperature and lattice temperature as a function of depth at 200 fs heated by a laser pulse with $t_{\rm p}$ of 50 fs and J_0 of 40 J/cm^2. The inset is the energy source term Q at the target surface as a function of time.

Based on the result in Fig. 2, we further investigate the temporal evolution of the material temperature at different depths, and it is found that the temperature evolution in the depth range of 80 nm to 130 nm is different from that on the target surface. In this case, the result at a depth of 100 nm, as shown in Fig. 3, is chosen for the representative to discuss the characteristics of the temperature evolution in this depth range. Since the temperature of the electrons on the upper layer is higher after the laser pulse, the temperature of the electrons on this layer will increase due to the thermal conduction of the electrons; at the same time, electrons transfer the energy to the lattice on this layer through the electron–phonon coupling effect, leading to a decrease of the electron temperature on this layer. After laser irradiation, the thermal conduction of the electrons could induce a decrease in the temperature gradient and consequently an attenuation of the thermal conduction of electrons. On the other hand, since the increasing rate of the electron temperature is faster than the counterpart of the lattice temperature for the larger thermal conductivity of the electrons, the difference between the electron temperature and the lattice temperature will decrease gradually, leading to the enhancement of the electron–phonon coupling effect. When the thermal conduction of electrons and the electron–phonon coupling are in equilibrium with each other, the electron temperature reaches the maximum value of 1.44×10^5 K.

Figure 3 also shows that the electron temperature at the depth of 100 nm at the end of the pulse is 5.46×10^4 K, namely, the temperature increases to 5.46×10^4 K due to the absorption of the laser energy. This value is much smaller than the maximum electron temperature of 1.44×10^5 K, which indicates that the contribution of the absorption of the laser energy to the temperature increase is not dominant at a depth greater than 80 nm, and the temperature is

mainly influenced by the thermal conduction of free electrons instead. The ablation depth in such experimental conditions could be ~ 1 μm,[6], which is much greater than 80 nm, and therefore it can be concluded that the material ablation in such a case is mainly induced by the thermal conduction of the electrons.

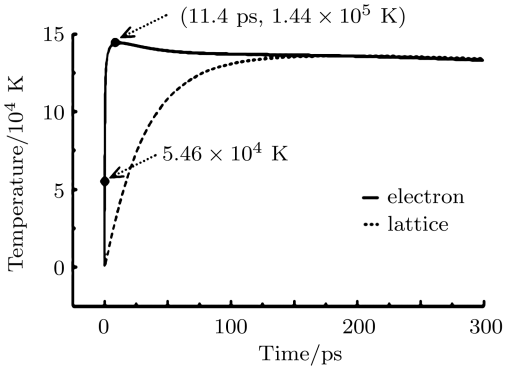


Fig. 3. Electron and lattice temperature as a function of time at a depth of 100 nm heated by a laser pulse with $t_{\rm p}$ of 50 fs and J_0 of 40 J/cm^2.

When the depth exceeds 130 nm, the evolution of the electron temperature and lattice temperature is found to be different from that at the target surface and that in the depth range of 80 nm to 130 nm. In this case, we choose the results at a depth of 500 nm, as shown in Fig. 4, for the representativeness to discuss the temperature evolution in this depth range. It is noticed in Fig. 4(a) that the electron temperature reaches the maximum value of 7297 K at 7.26 ps, and then it decreases gradually and reaches the minimum value of 5710 K at 34.45 ps. Thereafter, both the electron temperature and the lattice temperature increase gradually.

The electron temperatures at depths greater than 210 nm are all equal to the room temperature of 300 K at the end of the laser pulse, as mentioned above, which indicates that the electrons at depths greater than 210 nm cannot directly absorb the laser energy. Therefore, the thermal process at a depth of 500 nm only contains the heat flow of free electron and electron–phonon coupling. In order to investigate the relation between the two, we calculated the term of electron heat flow $(\partial k_{\rm e}/\partial z)(\partial T_{\rm e}/\partial z)$ and the term of electron–phonon coupling $G(T_{\rm e}–T_{\rm l})$, respectively, as shown in Fig. 4(b). The two curves in Fig. 4(b) converge at 7.26 ps and 34.45 ps, which correspond to the point of the maximum electron temperature and the minimum electron temperature in Fig. 4(a), respectively. This indicates that the electron temperature reaches the extreme values when the heat flow of the free electrons and electron–phonon coupling are in equilibrium with each other.

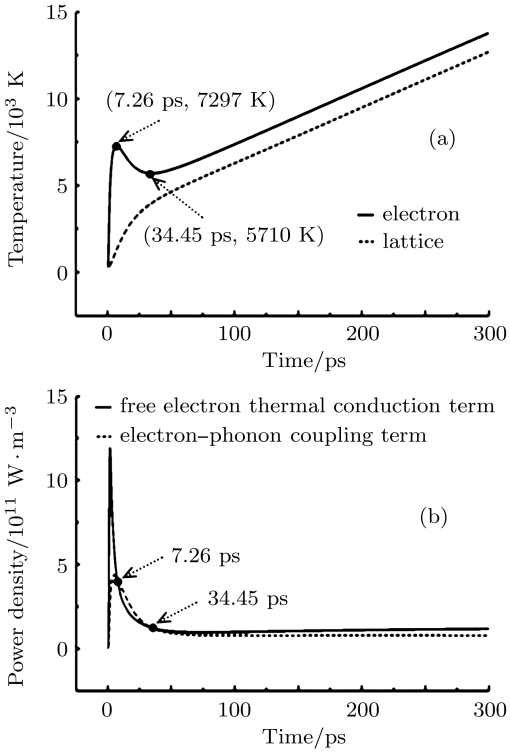


Fig. 4. (a) Electron and lattice temperature as a function of time. (b) The heat flow of the free electron and electron–phonon coupling term as a function of time, at a depth of 500 nm inside the aluminum target.

According to Figs. 4(a) and 4(b), the thermal process at a depth of 500 nm can be divided into the following three stages.

The first stage is from the laser pulse end to 7.26 ps. In this stage, the effect of electron heat flow is stronger than the effect of electron–phonon coupling, and thus the electron temperature increases sharply. At the same time, the difference between the electron temperature and the lattice temperature increases rapidly, leading to an enhancement of the electron–phonon coupling effect. With the development of thermal conduction, the heat flow of the free electron is damped gradually, and it is in equilibrium with electron–phonon coupling at 7.26 ps, at this time the electron temperature reaches the maximum value of 7297 K.

The second stage is from 7.26 ps to 34.45 ps. In this stage, the effect of electron–phonon coupling, in contrast, is stronger than the effect of electron heat flow, which leads to a decrease in the electron temperature. However, the lattice temperature increases continuously at this stage. Therefore, the difference between the electron temperature and the lattice temperature decreases, leading to the damping of the

electron–phonon coupling effect. The electron heat flow is in equilibrium with the electron–phonon coupling effect again at 34.45 ps, and the electron temperature reaches a minimum value of 5710 K at this time.

The third stage is after 34.45 ps. At this stage, the term of electron heat flow is slightly greater than the term of electron–phonon coupling, and thus both the electron temperature and the lattice temperature increase gradually.

4. Conclusion

In this paper, the implicit finite difference method is employed to numerically solve the two-temperature equation for the electron and lattice temperatures over a larger tempo-spatial range in the intense femtosecond laser ablation process of an aluminum target. Based on the analyses of the results, it is concluded that the characteristics and physical mechanisms of the evolution of electron temperature at different depths are different, as summarized below.

(i) The electron–phonon relaxation time is much longer than the pulse duration in the intense femtosecond laser ablation of aluminum.

(ii) The absorption of laser energy can only dominate the temperature increase in the laser heated material in a small depth range, while that in other ranges is mainly induced by the thermal conduction of free electrons, which indicates that the intense femtosecond laser ablation is mainly induced by the thermal conduction of the free electrons.

(iii) Affected by the heat flow of the free electrons and the electron–phonon coupling, the temperature of the free electrons deep inside the target will experience a process of increase followed by a decrease, before it finally increases with that of the lattice.

The above conclusions go beyond the particular case of aluminum and can be extended to the cases of other metals, due to the similarity of thermal properties among metals.

Acknowledgements

The authors would like to thank Li Lu-Jie and Ma Zhong-Hong for their critical reading of the manuscript.

References

[1] Nolte S, Momma C, Jacobs H, Tunnermann A, Chichkov B N, Wellegehausen B and Welling H 1997 *J. Opt. Soc. Am.* B **14** 2716

[2] Yang J J, Liu W W and Zhu X N 2007 *Chin. Phys.* **16** 2003

[3] Hu D Z 2009 *Acta Phys. Sin.* **58** 1077 (in Chinese)

[4] Ni X C, Wang Q Y and Liang J G 2006 *Acta Phononica Sin.* **35** 1 (in Chinese)

[5] Harzic R L E, Breitling D, Weikert M, Sommer S, Fohl C, Dausinger F, Valette S, Donnet C and Audouard E 2005 *Appl. Phys.* A **80** 1589

[6] Colombier J P, Combis P, Bonneau F, Harzic R L and Audouard E 2005 *Phys. Rev.* B **71** 165406

[7] Anisimov S I, Kapeliovich B L and Perelman T L 1974 *Sov. Phys. JETP* **39** 375

[8] Gamaly E G, Madsen N R, Golberg D and Rode A V 2009 *Phys. Rev.* B **80** 184113

[9] Chichkov B N, Momma C, Nolte S, von Alvensleben F and Tunnermann A 1996 *Appl. Phys.* A **63** 109